Path-integral simulation of positronium in a hard sphere

Zhi-Hua Liu
Materials Science Department, State University of New York, Stony Brook, New York 11794

Jeremy Broughton*
Materials Science Department, State University of New York, Stony Brook, New York 11794
and Complex Systems Theory Branch, Naval Research Laboratories, Washington, D.C. 20375
(Received 16 September 1988)

We employ the path-integral Monte Carlo method to study the binding energy of positronium trapped within a hard sphere. The two-body density matrix and the total- and kinetic-energy matrices are obtained by matrix squaring. The pair-product approximation is then used to obtain the entire density and estimator matrices for the Monte Carlo simulation. Ground-state binding energies are obtained as a function of sphere radius and the system is found to become unbound near a radius of 4 bohrs. Annihilation times are calculated which vary from 125 ps for free-space positronium down to 76 ps at a sphere radius of 4 bohrs.

I. INTRODUCTION

Since the first discovery of positronium, the localization of positronium in molecular media has attracted both theoretical and experimental interest.[1,2] In molecular liquids and dense gases, positronium can be trapped in a cavity where the medium's atoms are pushed away by the exchange repulsion interaction between the positronium's electron and the medium's electrons. This phenomenon has been observed in He,[3–7] Ne,[5] Ar,[8] H_2,[9] and many other organic liquids and gases.[10] Accompanying the positronium trapping, the positronium lifetime is increased sharply and shows a nonlinear relationship with the medium's density. This phenomenon is known as "positronium bubble" formation by analogy with the "electron bubbles" observed in He fluid.

An important application of positron spectroscopies in molecular solids is the measurement of vacancy density and configuration. This is because positronium localized in vacancies and defect voids has annihilation rates which are sensitively related to void size and configuration. This is one of the classic ways to determine void sizes in nonmetallic crystals. Localized and delocalized positronium also have different lifetimes. The lifetime responds to changes in the structure of the material due to temperature,[11,12] pressure,[13] or external field.[14] This property has been used in the study of the dynamics of phase transitions.

A natural way to study positronium in complex dynamical systems is by path-integral simulation. The method is based upon Feynman's formulation of quantum mechanics.[15] As a precursor towards a direct study of positron and positronium solvated in liquid and defective crystalline inert-gas systems, we first investigate positronium within a hard-sphere system. This is, of course, a two-quantum-particle problem with no exchange which can be treated rather simply by path integrals. In Sec. II we describe the path-integral Monte Carlo algorithm. Section III gives our results first for free positronium, then for a particle (with mass equal to that of the electron) in hard spheres of different sizes, and finally for positronium in those same spheres. Section IV presents our conclusions.

II. ALGORITHM

The density matrix (K) of an N-particle system at temperature T is given by

$$K(\mathbf{R},\mathbf{R}';\beta)=\sum_i \phi_i(\mathbf{R})\phi_i^*(\mathbf{R}')\exp(-\beta E_i)\ , \tag{1}$$

where i labels states of the system, ϕ are eigenfunctions, E is energy, and β is $(1/kT)$. $\mathbf{R}$ refers to the $3N$-particle coordinates. All static properties of the system are obtainable from the density matrix which satisfies the identity

$$K(\mathbf{R},\mathbf{R}';\beta)=\int\cdots\int d\mathbf{R}_1\cdots d\mathbf{R}_{M-1} \times K(\mathbf{R},\mathbf{R}_1;\tau)\cdots K(\mathbf{R}_{M-1},\mathbf{R}';\tau)\ , \tag{2}$$

where $\tau=\beta/M$ and M can be any integer. $K(\tau)$ is the density matrix at the higher temperature MT. This multidimensional integral can be evaluated by the Monte Carlo method if the integrand is known. When M is sufficiently large, $K(\tau)$ can be approximated by its classical form,

$$K(\mathbf{R},\mathbf{R}';\tau)=K^0(\mathbf{R},\mathbf{R}';\tau) \times\exp\{-\tau/2[V(R)]+V(R')\}\ , \tag{3}$$

where K^0 is the free-particle density matrix

$$K^0(\mathbf{R},\mathbf{R}';\tau)=(m/2\pi\tau h^2)^{-3/2}\exp\left[\frac{-m(\mathbf{R}-\mathbf{R}')^2}{2\tau h^2}\right]\ . \tag{4}$$

In this so-called primitive algorithm each quantum particle is represented as a necklace of M classical beads in which each bead interacts with only its nearest neighbors via a harmonic potential (which depends upon temperature) and with a reduced external field of $V(R)/M$. It is thereby possible to implement Monte Carlo importance sampling algorithms (we used the Metropolis scheme) to treat quantum many-body systems via a classical analog. The necklace analogy makes it clear that these (distinguishable) quantum systems are M times more computationally burdensome than the equivalent classical systems because of the typically slow convergence of path integrals. The situation is even worse when exchange effects are included in the study of boson or fermion systems.

What is required is an algorithm which reduces M and yet adequately describes the quantum nature of the particles in the system. One way of determining how important quantum effects are likely to be is through the thermal de Broglie wavelength:

$$\lambda=(h^2/mkT)^{1/2} . \tag{5}$$

If λ is small compared with relevant length scales (d) in the system, such as mean atomic distances or length scales of potential energy variation in accessible parts of configuration space, then the system may be treated classically. The order of M to adequately describe a quantum particle can be estimated by

$$M \simeq (\lambda/d)^2 , \tag{6}$$

where d is the length scale described above and M increases as temperature decreases.

For a single quantum particle in a smooth potential field, the number of beads needed is small, and the primitive algorithm is sufficient to get good convergence. Many realistic problems have been studied by this method such as the excess electron in molten KCl,[16] in helium,[17] and in water,[18–20] muonium in H_2O,[21] and negatively charged NaCl clusters.[22] For pathological systems, however, such as quantum particles in coarse potential media at low temperature, the number of beads needed in the primitive algorithm is too large to get good convergence. For the attractive Coulomb system the primitive algorithm fails completely; the singularity at the origin cannot be handled by a finite number of beads. One way to reduce the bead number is to include higher-order terms in the Trotter expansion for the density matrix.[23,24] This method has been applied to the ground state of the hydrogen atom[24] and to the study of helium phase transitions on graphite.[25] In another approach a staging algorithm, involving primary and secondary necklaces, has been developed by Sprik, Klein, and Chandler[26] to increase the efficiency of Monte Carlo sampling in the study of systems with strong short-ranged repulsive interactions. The method has been applied to the solvated electron in hard spheres[27] and liquid ammonia.[28]

An alternative way of reducing the number of beads is to use the quantum effective potential instead of the classical potential in the high-temperature approximation [Eq. (3)]. The matrix-squaring method,[29] which is an accurate and efficient method for obtaining the two-body density matrix, provides the means to produce an effective potential from the diagonal terms of the density matrix. The off-diagonal terms and the property estimators may be obtained from those on the diagonal via the end-point approximation.[30] The entire density matrix may then be constructed using the pair-product approximation

$$K(\mathbf{R},\mathbf{R}';\beta)=\prod_i K^0(\mathbf{r}_i,\mathbf{r}'_i;\beta)\prod_{i<j}\tilde{K}(\mathbf{r}_{ij},\mathbf{r}'_{ij};\beta) , \tag{7}$$

where $\mathbf{r}$ represents atomic coordinates and $\tilde{K}$ represents the normalized pair density matrix

$$\tilde{K}(\mathbf{r}_{ij},\mathbf{r}'_{ij};\beta)=K(\mathbf{r}_{ij},\mathbf{r}'_{ij};\beta)/K^0(\mathbf{r}_{ij},\mathbf{r}'_{ij};\beta) . \tag{8}$$

In the study performed here, however, we use matrix squaring and the pair-product approximation, but instead of the end-point approximation, the entire two-body density matrix is employed. We find that we need to do this to describe positronium properly. Ceperley and Pollock,[31] in their paper on the superfluid transition of liquid helium also used off-diagonal elements of the density matrix but parametrized to a low-order expansion in $(\mathbf{r}-\mathbf{r}')$.

The idea, then, is to matrix square down to a temperature (T_{med}) at which the pair-product approximation is good and then, using the contents of the resulting density matrices, to employ Monte Carlo simulation to take us to the temperature of interest (T_{fin}).

The matrix-squaring method follows directly from Eq. (2) which is exact. The two-body density matrix at temperature T can be obtained by numerical multiplication of the two identical density matrices representative of twice T,

$$K(\mathbf{r},\mathbf{r}';\beta)=\int d\mathbf{r}_1 K(\mathbf{r},\mathbf{r}_1;\beta/2)K(\mathbf{r}_1,\mathbf{r}';\beta/2) . \tag{9}$$

Starting at high temperature T_{hi} at which K may be approximated by its classical expression [i.e., akin to Eq. (3)], after p iterations of matrix squaring, we end up with the density matrix for the lower temperature $T_{\text{hi}}/2p$. Larger and larger values of p and different mesh sizes may be tried until the resulting density matrices at T_{med} become invariant.

Turning now to the estimator matrix and noting that the total energy of a system is given by

$$E_{\text{tot}}=-\frac{1}{Z}\frac{dZ}{d\beta} , \tag{10}$$

where Z is the partition function obtained from the full density matrix and that the kinetic energy is given by

$$KE=-\frac{m}{\beta Z}\frac{dZ}{dm} , \tag{11}$$

we define the following total-energy estimator matrix:

$$E(\mathbf{r},\mathbf{r}';\beta)=\frac{dK(\mathbf{r},\mathbf{r}';\beta)}{d\beta} \tag{12}$$

and kinetic energy estimator matrix,

$$KE(\mathbf{r},\mathbf{r}';\beta)=\frac{dK(\mathbf{r},\mathbf{r}';\beta)}{dm} . \tag{13}$$

These estimator matrices (EM) satisfy

$$\mathrm{EM}(\mathbf{r},\mathbf{r}';\beta)=\tfrac{1}{2}\int d\mathbf{r}_1[\mathrm{EM}(\mathbf{r},\mathbf{r}_1;\beta/2)K(\mathbf{r}_1,\mathbf{r}';\beta/2) +K(\mathbf{r},\mathbf{r}_1;\beta/2)\mathrm{EM}(\mathbf{r}_1,\mathbf{r}';\beta/2)] . \tag{14}$$

Again, in determining system properties, the full estimator matrix, including both the diagonal and off-diagonal terms, is employed. Starting at the same high temperature as the density matrix, p iterations of matrix squaring were performed to obtain the estimator matrices for the lower temperature of $T_{\mathrm{hi}}/2p$.

To order to simplify the calculations, the three-dimensional density matrix can be reduced to a sum of one-dimensional matrices by the following l-partial wave expansion:

$$K(r,r';\beta)=\sum_{l=0}^{\infty}\frac{2l+1}{4\pi rr'}k_l(r,r';\beta)P_l(\cos\theta) , \tag{15}$$

where θ is the angle between $\mathbf{r}$ and $\mathbf{r}'$ and $P_l(x)$ are Legendre polynomials. Each k_l obeys analogous matrix squaring relationships to Eq. (9) as do the l partial wave expansions for the energy estimators.

The potential energy estimator is obtained as the simple ensemble average of the potential energy (PE) between particles in the system. Thus, we have independent methods for obtaining potential, kinetic, and total energies and are able to determine internal consistency between the values of all three.

III. RESULTS

In the ensuing, energy is given in Rydbergs, distance in bohrs, and temperature in Kelvin. For positronium, Monte Carlo steps involve moving pairs of beads at a time, that is, an electron and a positron bead and the relative distance between them. We found that many bead moves, such as moving the center of mass of a necklace, or moves associated with the normal modes of a necklace, had negligible effect on the quality of the estimator statistics.

A. Free positronium

It is impossible to simulate the hydrogen atom by the primitive Monte Carlo algorithm because the Coulombic potential is pathological. The beads collapse into the nucleus because of the singularity in the potential. The high-order Trotter expansion[24] for the density matrix has been used to handle this problem but the convergence with bead number is very slow. Storer[32] showed, using the **S** partial wave matrix-squaring method, that it was possible to obtain diagonal terms of the density matrix and hence the quantum effective potential. Here, however, we used the l partial wave expansion for the positronium problem:

$$K_l(r,r';\beta)\simeq\int_0^R dr_1\, k_l(r,r_1;\beta/2)k_l(r_1,r';\beta/2) , \tag{16}$$

where R is chosen sufficiently large (12 bohrs) that it has minimal effect (less than 0.1%) on the value of k_l in regions of high probability in phase space. Sufficient partial waves, depending upon T_{med}, are included in the sum of Eq. (15) to make K converge. For the range of T_{med} values studied here, this upper limit on l was 40.

In Table I the ground state energy of free positronium is evaluated. Starting the matrix squaring at $T_{\mathrm{hi}}=2^{13}\times10^4$ K, Table I shows the effect of different values of T_{med} on the numerical accuracy achieved through Monte Carlo simulations. We know that the system is in its ground state at 10^4 K, and this is the temperature at which we run the Monte Carlo code. As expected, the root-mean-square energy fluctuation increases with bead number (i.e., T_{med}), and this is why there appears to be an M dependence to the results despite the fact that we are using the exact density matrix. Even though this system is unbounded at any finite T ($\langle R\rangle$ is infinite), the electron-positron pair was never observed to separate during the course of the simulation.

B. Particle in a hard sphere

As discussed by Barker,[33] the primitive Monte Carlo algorithm is not suitable for the hard-potential-well problem. In order to satisfy the boundary condition at the

TABLE I. The ground-state energy of free positronium as a function of the medium temperature T_{med}. The radial mesh size is 0.075, and the angular mesh size needed to accurately express the angular terms increases as T_{med} increases.

T_{med} (K)	E (Ry)	KE (Ry)	PE (Ry)	M
0.4×10^5	-0.4994 ± 0.0002	0.4952 ± 0.0011	-0.960 ± 0.014	4
0.8×10^5	-0.4990 ± 0.0002	0.4940 ± 0.0013	-0.954 ± 0.007	8
1.6×10^5	-0.4991 ± 0.0006	0.4938 ± 0.0030	-0.973 ± 0.005	16
3.2×10^5	-0.4995 ± 0.0021	0.4897 ± 0.0053	-0.970 ± 0.009	32
6.4×10^5	-0.4990 ± 0.0060	0.4809 ± 0.0119	-0.966 ± 0.019	64
12.8×10^5	-0.5243 ± 0.0165	0.4804 ± 0.0278	-0.957 ± 0.030	128
	-0.5000	0.5000	-1.000	

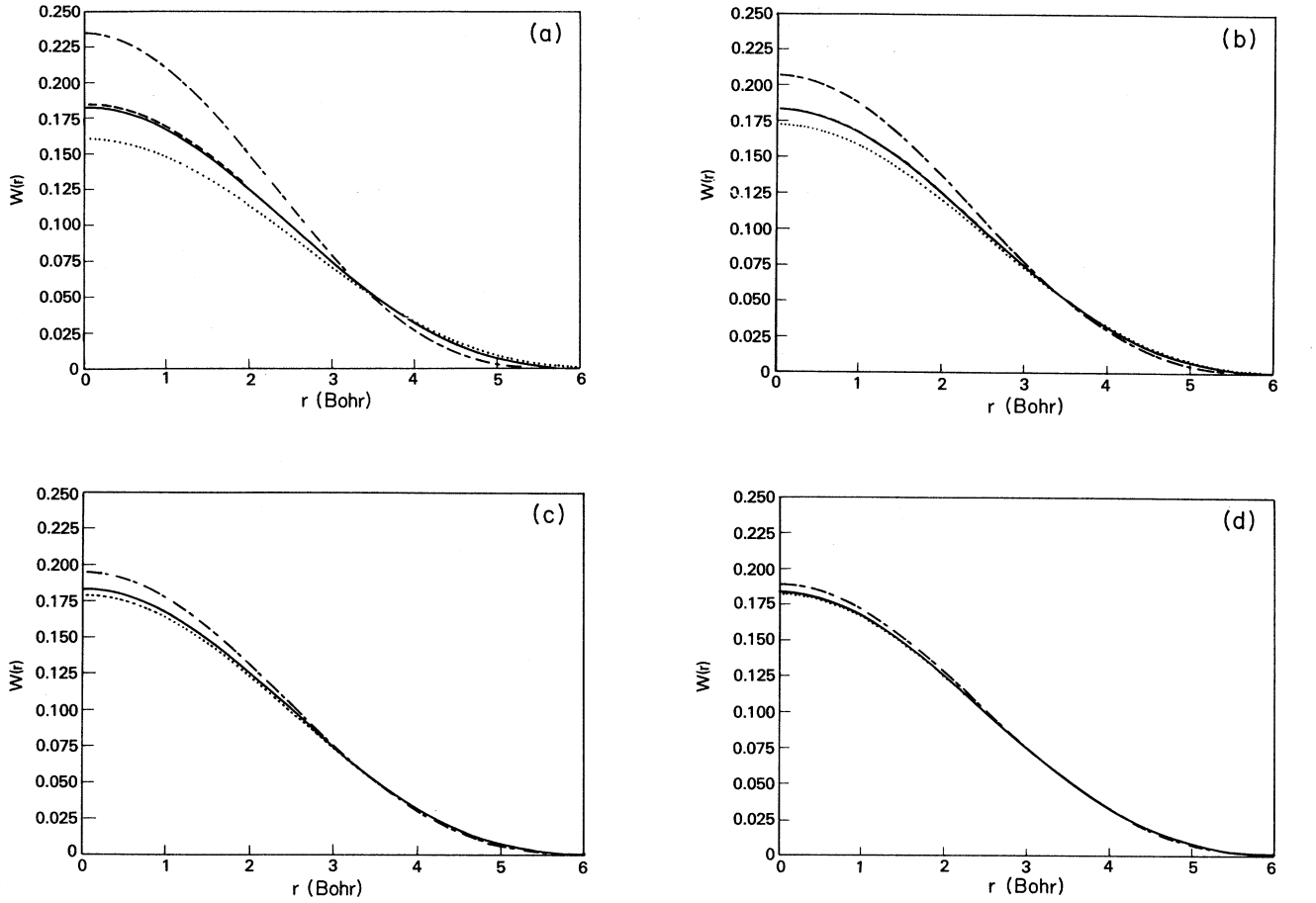

FIG. 1. Ground-state wave function of an electron in a hard sphere of radius 6 bohrs for different starting matrix-squaring temperatures (T_0). Exact wave function (solid line); image approximation Eq. (18) (dashed line); image approximation Eq. (17) (dash-dotted line); and semiclassical approximation Eq. (3) (dotted line). (a) $T_{hi}=512\times10^4$ K; (b) $T_{hi}=2048\times10^4$ K; (c) $T_{hi}=8192\times10^4$ K; (d) $T_{hi}=32\,768\times10^4$ K. $T_{med}=0.5\times10^4$ K in each case.

wall, he used the one-dimensional image approximation to correct the high-temperature density matrix and was able to reduce the number of beads required for accurate solution of the problem.

TABLE II. The ground-state energy of one quantum particle (mass of an electron) in a hard-sphere potential well of radius 6.0 bohr for various T_{med}. The radial mesh size is 0.075, and the angular mesh size increases as T_{med} increases. l_t represents the total number of partial waves included in the sum for the pair matrices [Eq. (15)].

T_{med} (K)	E (Ry)	l_t	M
0.4×10^5	0.2747±0.0001	10	4
0.8×10^5	0.2744±0.0003	10	8
1.6×10^5	0.2742±0.0022	10	16
3.2×10^5	0.2726±0.0044	20	32
6.4×10^5	0.2732±0.0063	20	64
12.8×10^5	0.2747±0.0084	30	128
	0.2742		

In the present calculation, we have investigated two forms of image approximation for use within the hard sphere. The first is due to Jacucci and Omerti[34] and the second to Whitlock and Kalos:[35]

TABLE III. The ground-state binding and potential energy of positronium in a hard sphere of radius 8.0 bohr at different values of T_{med}. The ground-state binding energy converges as the pair-product approximation becomes more accurate with increasing T_{med}. The error caused by the fluctuation increases as the number of beads in the Monte Carlo simulation increases.

T_{med} (K)	E (Ry)	PE (Ry)
0.4×10^5	−0.276±0.001	−1.095±0.013
0.8×10^5	−0.324±0.002	−1.057±0.011
1.6×10^5	−0.360±0.005	−1.037±0.016
3.2×10^5	−0.386±0.016	−1.046±0.030
6.4×10^5	−0.399±0.013	−1.034±0.014

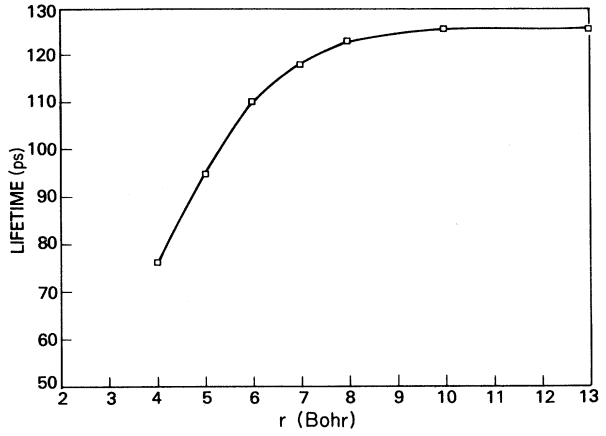

FIG. 2. The 2γ-annihilation lifetime of positronium as a function of sphere radius.

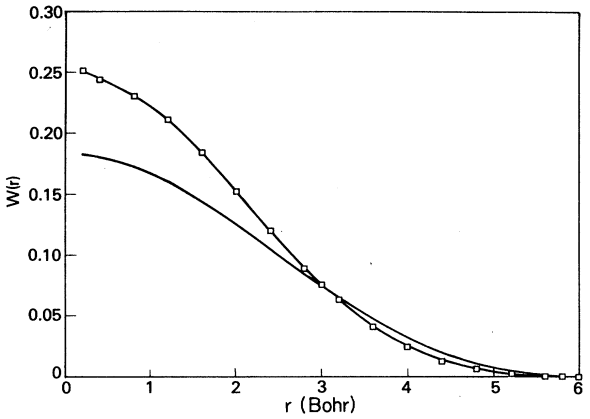

FIG. 3. Comparison of the electron ground-state wave function in the positronium hard-sphere system (squares) with that of a single electron (solid line) in a hard sphere of the same size.

$$K(\mathbf{r},\mathbf{r}';\beta)=K^0(\mathbf{r},\mathbf{r}';\beta)\left[1-\exp\left[-\frac{(R_0-r)(R_0-r')}{2\beta}\right]\right], \tag{17}$$

$$K(\mathbf{r},\mathbf{r}';\beta)=K^0(\mathbf{r},\mathbf{r}';\beta)\left[1-\exp\left[-\frac{(R_0^2-r^2)(R_0^2-r'^2)}{2\beta R_0^2}\right]\right], \tag{18}$$

where R_0 is the sphere radius. We assume the mass of the sphere to be infinite and the mass of the particle to be that of the electron. These equations are used to start the matrix squaring. Because matrix squaring can start at very high temperatures, the image approximation only affects a narrow region near the hard-sphere wall at these temperatures. Differences near the hard wall at high temperature propagate to have a profound influence on the wave function at the center of the sphere at T_{med} and/or T_{fin}. This effect is demonstrated in Fig. 1 for a hard-sphere radius of 6 bohrs, where the image approximation of Eq. (18) is found to be superior. The diagonal terms of the ground-state density matrix can actually be obtained accurately (i.e., compared with the known exact answer) by starting at high enough temperature and omitting the image approximation. The difference in the final density matrix between starting with just the classical or with the image approximation is less than the numerical error associated with matrix squaring (i.e., the use of the trapezium rule in the integration) itself under these circumstances.

At the temperature at which we start our matrix squaring, the image approximation given by Eq. (18) provides the initial matrix. Table II presents values for the total energy for different values of T_{med} for a sphere of radius 6 bohrs. Again, the starting temperature is $T_0=2^{13}\times10^4$ K and the final (i.e., close to ground state) temperature is 10^4 K. The exact ground-state energy is 0.2742. The upper limit on the number of partial waves included was 30. Again, we note that the root-mean-square fluctuation in energy grows with bead number.

C. Positronium in a hard sphere

Positronium in a hard sphere is a three-body problem and may be handled by making the pair-product approximation to the density matrix. The hard sphere is taken to have infinite mass. For each sphere radius it is necessary to find the value of T_{med} for which the pair-product ap-

TABLE IV. The ground-state binding energy, kinetic energy, and potential energy of positronium in a hard sphere as a function of T_{med} for sphere radius of 10.0 bohr. The result is consistent with E equal to the sum of the kinetic and potential energies within the statistical errors.

T_{med} (K)	E (Ry)	PE (Ry)	KE (Ry)	E-PE (Ry)
0.4×10^5	-0.372 ± 0.002	-1.019 ± 0.008	0.643 ± 0.004	0.647
0.8×10^5	-0.407 ± 0.002	-1.018 ± 0.008	0.608 ± 0.006	0.611
1.6×10^5	-0.423 ± 0.007	-1.016 ± 0.008	0.590 ± 0.009	0.593
3.2×10^5	-0.427 ± 0.008	-1.013 ± 0.013	0.582 ± 0.012	0.586

TABLE V. Binding energy and potential energy of ground-state positronium inside hard spheres of different radii. T_p is the minimum temperature at which the pair-product approximation is valid. This determines the number of beads required to reach the ground state. T_p increases as the sphere radius decreases; hence, the statistical fluctuation increases also. For sphere radii smaller than 4.0 bohr, the fluctuation is larger than the magnitude of the binding energy. The last column is the energy (E_{ref}) of unperturbed positronium in a hard sphere (see text).

R (bohrs)	E (Ry)	PE (Ry)	T_p (K)	E_{ref} (Ry)
4.0	−0.026±0.046	−1.299±0.041	2.56×10^6	−0.192
5.0	−0.151±0.023	−1.177±0.023	2.56×10^6	−0.303
6.0	−0.227±0.025	−1.120±0.029	1.28×10^6	−0.363
7.0	−0.349±0.013	−1.061±0.021	1.28×10^6	−0.399
8.0	−0.399±0.013	−1.034±0.014	0.64×10^6	−0.423
10.0	−0.427±0.008	−1.009±0.008	0.32×10^6	−0.451
13.0	−0.453±0.003	−1.000±0.009	0.08×10^6	−0.471
	−0.500	−1.000		−0.500

proximation is valid. T_{med} increases, of course, with decreasing radius size. Thus, the bead number in the Monte Carlo part of the calculation increases with decreasing sphere size. The greatest estimator noise is therefore found for small spheres.

Table III demonstrates this point. The energies and potential energies converge (i.e., differences are in the noise) after 64 beads for a sphere radius of 8 bohrs. Table IV shows that at the larger radius of 10 bohrs, 32 beads are required for convergence. Further, the kinetic, potential, and total-energy estimators are compared and found to be internally consistent. Finally, Table V presents total energy as a function of sphere size. The kinetic energy becomes equal to the potential energy near a radius of 4 bohrs. Also included is a column involving the sum of the total energy of free positronium and the kinetic energy of a particle of two electron masses as a function of a hard-sphere size. This would be the energy of the system if the positronium wave function was unperturbed by the presence of the hard sphere. Comparison of this column with the second indicates that very significant changes are occurring in the positronium at radii less than 7 bohrs, a fact corroborated by the positronium lifetime data given below.

Annihilation rates (P_A) may be found from the following approximate equation:

$$P_A=\pi c r_e^2 n_e \ , \tag{19}$$

where r_e is the classical electron radius, c is the velocity of light, and n_e is the electron density at the positron origin. The probability density as a function of relative electron-positron coordinate was extrapolated to its origin to obtain n_e. Table VI presents lifetime results as a function of sphere size. We note that the lifetimes vary by a factor of 2 for the sphere sizes considered and that it asymptotes to the exact free-space value. The lifetime decreases rapidly for small-sphere radii as shown in Fig. 2.

Last, we present two figures to illustrate changes in probability density behavior from related reference systems. Figure 3 compares the wave function of a single electron in a hard sphere with that of the electron in positronium in the same sized (6 bohrs) sphere. The presence of the oppositely charged particle causes an increase in density at the center of the sphere. Figure 4 demonstrates the effect of containment on the relative positroni-

TABLE VI. The 2γ-annihilation lifetime of positronium as a function of sphere size. It asymptotes to the free positronium value as the sphere radius increases.

R (bohrs)	Lifetime (ps)
4.0	76±8
5.0	94±5
6.0	110±4
7.0	118±3
8.0	123±3
10.0	125±3
13.0	125±3
Free Positronium	125.0

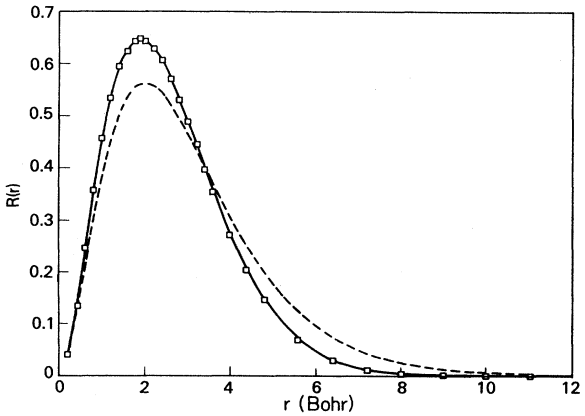

FIG. 4. Radial distribution function of positronium in a hard sphere (solid line) as compared with that of free positronium (dashed line).

um wave function. The maximum in the radial probability density increases in height but moves very little towards the origin.

IV. CONCLUSION

We have seen that it is possible to accurately represent positronium behavior in hard spheres of differing radii down to 4 bohrs using combined matrix-squaring and path-integral Monte Carlo techniques. Annihilation lifetimes vary from 125 ps at a radius size of 13 bohrs down to 76 ps at the smallest radii. We are now in a position to study positronium bubbles in inert-gas liquids and positronium localization at crystal vacancies using similar techniques.

ACKNOWLEDGMENTS

Z-H.L. wishes to thank the U.S. Department of Energy (Grant No. DE-FG02-85ER45218) for support during this work. Calculations were performed on machines purchased under Department of Energy (DOE) Grant No. DE-FG02-85ER45218 and under National Science Foundation (NSF) Grant No. DMR-8507628.

---

*Also at Sachs/Freeman Associates Inc., Landover, MD 20785-5396.

[1]W. Brandt and A. Dupasquier, *Positron Solid-State Physics* (North-Holland, New York, 1983).
[2]P. Hautojarvi, *Positrons in Solids* (Springer-Verlag, New York, 1979).
[3]L. O. Roelling and T. M. Kelly, Phys. Rev. Lett. **18**, 387 (1967).
[4]W. W. Walker and D. C. Cline, J. Chem. Phys. **60**, 4990 (1974).
[5]K. F. Canter, J. D. McNutt, and L. O. Roellig, Phys. Rev. A **12**, 375 (1975).
[6]P. Hautojarvi, K. Rytsola, P. Tuovinen, and P. Jauho, Phys. Lett. **57A**, 175 (1976).
[7]J. B. Smith, J. D. McGervey, and A. J. Dahm, Phys. Rev. B **15**, 1378 (1977).
[8]C. V. Briscoe, S. I. Choi, and A. T. Stewart, Phys. Rev. Lett. **20**, 493 (1968).
[9]J. D. McNutt and S. C. Sharma, J. Chem. Phys. **68**, 130 (1978).
[10]C. D. Beling and F. A. Smith, Chem. Phys. **49**, 417 (1980).
[11]W. W. Walker, W. G. Merritt, and G. D. Cole, J. Chem. Phys. **56**, 3729 (1972).
[12]B. V. Thosar, R. G. Lagu, V. G. Kulkarni, and G. Chandra, Phys. Status Solidi B **55**, 415 (1973).
[13]R. K. Wilson, P. O. Johnson, and R. Stump, Phys. Rev. **129**, 2091 (1963).
[14]W. Brandt and J. Wilkenfield, Phys. Rev. B **12**, 2579 (1975).
[15]R. P. Feynman and A. R. Hibbs, *Quantum Mechanics and Path Integrals* (McGraw-Hill, New York, 1965).
[16]M. Parrinello and A. Rahman, J. Chem. Phys. **80**, 860 (1984).
[17]J. Bartholomew, R. W. Hall, and B. J. Berne, Phys. Rev. B **32**, 548 (1985).
[18]C. D. Jonah, C. Romero, and A. Rahman, Chem. Phys. Lett. **123**, 209 (1986).
[19]P. J. Rossky, J. Schnitker, and R. Kuharski, J. Stat. Phys. **43**, 949 (1986).
[20]A. Wallquist, D. Thirumalai, B. J. Berne, and C. Pangali, J. Chem. Phys. **85**, 1583 (1986).
[21]B. DeRaedt, M. Sprik, and M. L. Klein, J. Chem. Phys. **85**, 1583 (1986).
[22]U. Landman, D. Scharf, and J. Jortner, Phys. Rev. Lett. **54**, 1860 (1985).
[23]M. Takahashi and M. Imada, J. Phys. Soc. Jpn. **53**, 3765 (1984).
[24]X. P. Li and J. Q. Broughton, J. Chem. Phys. **86**, 5094 (1987).
[25]F. F. Abraham and J. Q. Broughton, Phys. Rev. Lett. **59**, 64 (1987).
[26]M. Sprik, M. L. Klein, and D. Chandler, Phys. Rev. B **31**, 4234 (1985).
[27]M. Sprik, M. L. Klein, and D. Chandler, Phys. Rev. B **32**, 545 (1985); J. Chem. Phys. **83**, 3042 (1985).
[28]M. Sprik, R. W. Impey, and D. Chandler, J. Chem. Phys. **83**, 5802 (1985).
[29]A. D. Klemm and R. G. Storer, Aust. J. Phys. **26**, 43 (1973).
[30]E. L. Pollock and D. M. Ceperley, Phys. Rev. B **30**, 2555 (1984).
[31]D. M. Ceperley and E. L. Pollock, Phys. Rev. Lett. **56**, 351 (1986).
[32]R. G. Storer, J. Math. Phys. **9**, 964 (1967).
[33]J. A. Barker, J. Chem. Phys. **70**, 2914 (1979).
[34]G. Jacucci and E. Omerti, J. Chem. Phys. **79**, 9051 (1983).
[35]P. A. Whitlock and M. H. Kalos, J. Comput. Phys. **30**, 361 (1978).